Inorganic Chemistry

Article

The Nowotny Chimney Ladder Phases: Whence the 14 Electron Rule?

Daniel C. Fredrickson, Stephen Lee,* and Roald Hoffmann*

Department of Chemistry and Chemical Biology, Baker Laboratory, Cornell University, Ithaca, New York 14853-1301

The late transition metal Nowotny chimney ladder phases (NCLs, T_tE_m; T, groups 7–9; E, groups 13 and 14) follow a 14 electron rule: the total number of valence electrons per T atom is 14. In this paper, we extract a chemical explanation for this rule from extended Hückel calculations; we focus on $RuGa_2$, the parent NCL structure. A gap between filled and unfilled bands arises from the occupation of two Ga–Ga bonding/Ru–Ga nonbonding orbitals per $RuGa_2$, independent of *k*-point. In addition, the five Ru d levels are filled. Together this makes for 7 filled bands at each *k*-point, or 14 electrons per Ru. We discuss the connections between this 14 electron rule and the 18 electron rule of organometallic complexes.

1. Introduction

The Nowotny chimney ladders (NCLs) are a series of intermetallic compounds formed from transition (T) and main group (E) metals, named for an intriguing structural feature: the T atoms create 4-fold helices (in the shape of chimneys), inside of which the E atoms form separate helices.[1] Figure 1 shows two views ("top" and "side") of one of these phases, Ru_2Sn_3.[2] Note the chimney of the transition metal atoms and within it the 3-fold helix of the main group atoms.

A helix within a helix, what could be more beautiful? With a touch of sadness, a series of contributions will show that this perspective does not capture the electronic and structural richness of these phases.

Experimental work on the NCLs has led to a number of experimental rules. The first of these is a special stability associated with a total valence electron count of 14 electrons per T atom.[3,4] The second rule concerns the observation that the intensity of diffraction spots for an NCL T_tE_m follows the law that the main reflections are at intervals of $4t\mathbf{c}^*$ and that there are satellite spots at $(2t - m)\mathbf{c}^* = \mathbf{c}_{pseudo}$ around these main diffraction spots.[5–7]

Figure 1. The Ru_2Sn_3 structure type, an example of the Nowotny chimney ladder series. (a) A view down the **c** axis. (b) A perpendicular view illustrating the Ru and Sn helices. The Ru atoms are shown as red balls, while the Sn atoms are shown as blue balls. Heights are given in units of $\mathbf{c}_t$.

The second rule was explained in the first contribution of this series.[8] In this paper, we concentrate on the origin of first rule, the 14 electron rule. As a specific example we take the parent structure of the NCLs, TE_2, exemplified by $RuGa_2$. To anticipate our conclusion, we will find that throughout the Brillouin zone there are two Ga–Ga bonding levels whose shape leads to poor interaction with the transition metal d levels. The bands arising from these 2 orbitals are filled, along with the 5 d bands from the late transition metal, for a total of 7 bands or 14 electrons.

2. The $RuGa_2$ Structure

The structure of the archetypal Nowotny chimney ladder, $RuGa_2$, itself yields our first clues to the 14 electron rule.

* Authors to whom correspondence should be addressed. E-mail: sl137@cornell.edu (S.L.) or rh34@cornell.edu (R.H.).
 (1) Nowotny, H. Crystal Chemistry of Transition Element Defect Silicides and Related Compounds. In *The Chemistry of Extended Defects in Non-metallic Solids*; Eyring, L., O'Keeffe, M., Eds.; North-Holland Publishing Co.: Amsterdam and London, 1970.
 (2) Schwomma, O.; Nowotny, H.; Wittmann, A. *Monatsh. Chem.* **1964**, *95*, 1538−1543.
 (3) Jeitschko, W.; Parthé, E. *Acta Crystallogr.* **1967**, *22*, 417−430.
 (4) Pearson, W. B. *Acta Crystallogr.* **1970**, *B26*, 1044−1046.
 (5) Ridder, R. D.; Amelinckx, S. *Mater. Res. Bull.* **1971**, *6*, 1223−1234.
 (6) Ye, H. Q.; Amelinckx, S. *J. Solid State Chem.* **1986**, *61*, 8−39.
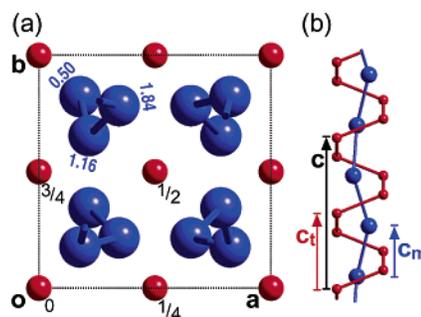 (7) Lu, G.; Lee, S.; Lin, J.; You, L.; Sun, J.; Schmidt, J. T. *J. Solid State Chem.* **2002**, *164*, 210−219.
 (8) Fredrickson, D. C.; Lee, S.; Hoffmann, R.; Lin, J. *Inorg. Chem.* **2004**, *43*, 6151−6158.
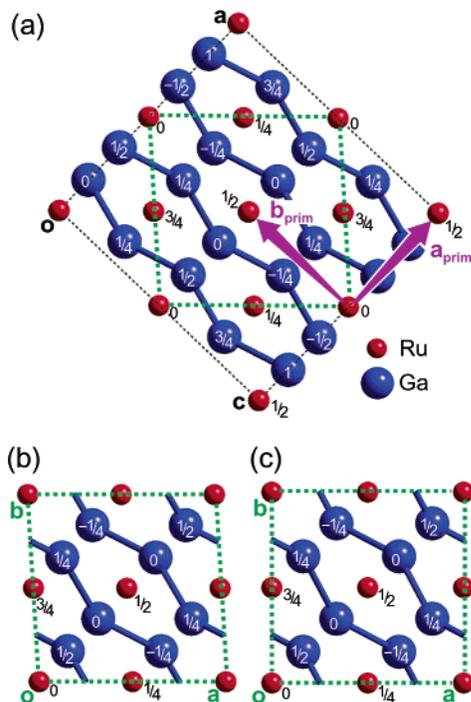
Figure 2. RuGa$_2$ in the TiSi$_2$ structure type. (a) The conventional face-centered unit cell for this structure. One choice of primitive cell vectors is indicated in purple (with one vector perpendicular to the plane of the page). (b) The unit cell analogous to the NCL structures. (c) The idealization of the RuGa$_2$ structure to be studied here. See footnotes 12 and 13 for a more detailed discussion.

Figure 3. The RuGa$_2$ structure viewed (a) as an NCL, helix within a helix, and (b) in another way, emphasizing the closest Ga–Ga contacts in the structure. Ru: red. Ga: blue.

Figure 4. The Ga coordination by other Ga atoms. This coordination forms a severely distorted trigonal bipyramid. (a) This trigonal bipyramid viewed roughly perpendicular to the axis of the trigonal bipyramid. (b) Viewed down the axis. The colors of the bonds, blue, yellow, and green, refer respectively to the three bond lengths of 2.57, 2.82, and 2.89 Å. Ru: red. Ga: blue.
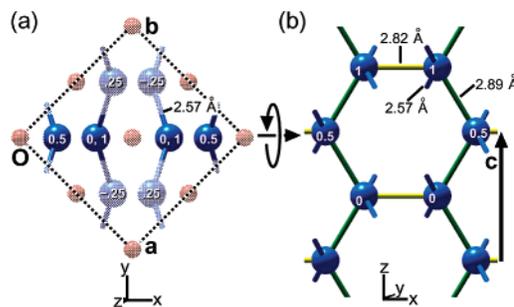
Figure 5. Contacts between the Ga chains. The closest Ga–Ga contacts between chains are contained within ($\overline{2}20$) layers in RuGa$_2$. (a) The RuGa$_2$ structure (rotated 45°) with one of these planes emphasized. (b) A [$\overline{2}20$] view of this layer, with the contacts between chains indicated with yellow and green bars.

RuGa$_2$ crystallizes in the TiSi$_2$ structure type.[9−11] We show this structure in Figure 2, where we isolate the unit cell that makes most clear the connection to the other NCL structures (Figure 2c).[12,13] As in the other NCLs, we are drawn to the helices. The 4-fold Ru (red) helices of RuGa$_2$, shaped like chimneys, are seen in Figure 3a as squares. Their helicity becomes apparent when we look at the heights: one turn of the helix emphasized in Figure 3a passes through heights 0, $^1/_4$, $^3/_4$, and 1**c**, rotating counterclockwise. The Ga atoms (blue) lie in the channels of the Ru network. They simply make zigzag chains, but in the other NCLs they are more intricate helices.

How important are these helices in terms of bonding? The Ru–Ru distance along the Ru helix is 3.29 Å, quite large compared to the average Ru–Ru distance in *hcp* Ru, 2.68 Å.[14] The distance between Ga atoms along the 2-fold helix

is 2.89 Å. Comparing this to the typical Ga–Ga single bond length of 2.5 Å, one expects that there is a substantial Ga–Ga interaction along the helix. Indeed there is, but for an understanding of the 14 electron rule, we must go further: the seductive helix description glosses over a rich set of Ga–Ga and Ru–Ga bonds.

A closer look at the distances reveals much more extensive Ga–Ga bonding. Each Ga atom has a severely distorted trigonal bipyramidal coordination by other Ga atoms (Figure 4). The two "axial" bonds are at 2.57 Å (blue), while the three "equatorial" bonds are longer: one at 2.82 Å (yellow) and two at 2.89 Å (green). The axial bonds join the Ga atoms into zigzag chains (Figure 3b). The equatorial bonds connect

(9) Jeitschko, W. *Acta Crystallogr.* **1977**, *B33*, 2347−2348.

(10) Jeitschko, W.; Holleck, H.; Nowotny, H.; Benesovsky, F. *Monatsh. Chem.* **1963**, *94*, 838−840.

(11) Evers, J.; Oehlinger, G.; Meyer, H. *Mater. Res. Bull.* **1984**, *19*, 1177−1180.

(12) The actual atomic coordinates for RuGa$_2$ have not been obtained experimentally, so we will use the coordinates for TiSi$_2$, with an adjustment of the cell parameters. As we described in our previous paper, this structure is in the space group *Fddd*, and is usually presented in terms of its face-centered cell, as is shown in Figure 2a. This cell is shown with black dotted lines. One choice of primitive cell vectors is indicated with purple arrows in Figure 2a.

(13) The **a** and **b** vectors for the experimental unit cell are not quite at a right angle to each other ($\gamma = 93.5°$). Since most of the other NCLs are tetragonal, and we are going to be constructing these other phases from RuGa$_2$ layers, we'll base our calculations on an idealized structure with $\gamma = 90°$ (this has little effect on the presence of the gap at 14 electrons per Ru atom). This idealized structure is shown in Figure 2c. The following analysis refers consistently to this idealized structure.
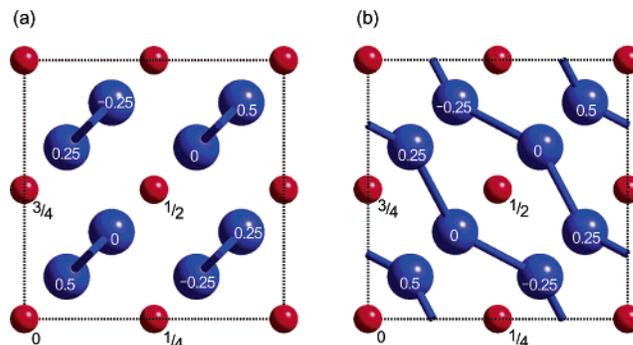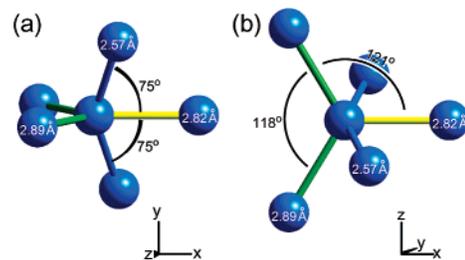
(14) Donohue, J. *The Structures of the Elements;* J. Wiley: New York, 1974.
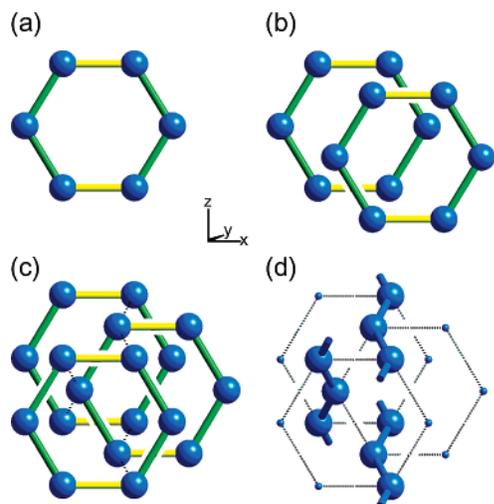
Figure 6. Stacking of Ga honeycomb nets in RuGa$_2$. (a) A Ga honeycomb net abbreviated as a single hexagon. (b) The stacking mode between adjacent Ga honeycombs, with the hexagons parallel, and the edge of the upper layer over the central void of the lower. (c) The stacking of three layers found in RuGa$_2$. The shortest Ga−Ga distances in the structure, at 2.57 Å, created by this stacking, are drawn in with black dotted lines. (d) The chains created from these contacts (those shown earlier in Figures 1 and 2b); the Ga−Ga contacts in the honeycomb nets are indicated with dotted lines. The colors of the Ga−Ga bonds are blue (d), yellow or green (a−c) for respectively the 2.57, 2.82, and 2.89 Å bonds. See Figure 4.
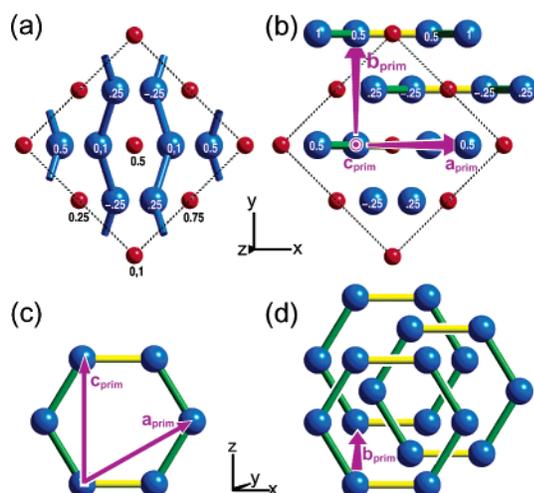

Figure 7. Building up RuGa$_2$ from the stacking of Ga honeycomb nets. (a) The RuGa$_2$ structure, with the Ga−Ga closest contacts indicated. (b) The RuGa$_2$ structure with the stacking of Ga honeycomb planes emphasized. **b**$_{prim}$ gives the smallest crystallographic repeat vector for the stacking. (c) A single hexagon of a Ga honeycomb, showing the RuGa$_2$ primitive cell axes **a**$_{prim}$ and **c**$_{prim}$. (d) The **b**$_{prim}$ axis connecting Ga honeycomb nets in the RuGa$_2$ structure. See Figure 4 for the significance of the blue, yellow, and green Ga−Ga bonds. Ru: red. Ga: blue.

the Ga atoms into honeycomb nets (Figure 5). Within the honeycomb nets, the 2.82 Å contacts form Ga pairs. The 2.89 Å ones form Ga zigzag chains along **c**, the "Ga helices" of Figure 3a.

Let's focus on the Ga honeycomb nets; they will make transparent important features of the RuGa$_2$ structure (and the orbitals coming later). We illustrate how they stack[4] in Figure 6, abbreviating the honeycomb layers as single hexagons. We start with a single layer (Figure 6a). Next we add new layers from above so that the hexagons are parallel, but offset so that an edge of the upper layer lies over the

hexagonal center of the lower (Figure 6b,c). This stacking creates the periodicity of the RuGa$_2$ structure (Figure 7). The primitive unit cell vectors **a**$_{prim}$ and **c**$_{prim}$ arise from the 2-dimensional periodicity of the honeycomb nets (Figure 7c). The third cell vector, **b**$_{prim}$, gives the repeat along the stack (Figure 7b,d).[15]

The shortest Ga−Ga contacts (the "axial" ones of the Ga trigonal bipyramids) link together the honeycomb nets along the stack. These contacts are shown in Figure 6c with black dotted lines between honeycombs. In Figure 6d we emphasize the duality of the Ga honeycombs and chains, drawing the Ga−Ga chains bonded between the nets with blue bars, and tracing out the honeycombs with black dotted lines. Both depictions of the Ga−Ga contacts will play a role as we delve into the electronic structure of this phase.

Now the Ru−Ga bonds: one Ru atom lies at the center of each hexagon of the Ga honeycombs, and this creates six Ru−Ga contacts, two at 2.90 Å, and four at 2.85 Å (Figure 8a). Two more Ga neighbors lie both above and below the Ru atom from the edges of the adjacent honeycomb layers of the stack (Figure 8b). These form the shortest of Ru−Ga contacts at 2.59 Å. These 10 Ga atoms create a Ru coordination environment of D_2 symmetry. The coordination environment of the Ga atoms is shown in Figure 8c, and is quite similar in shape. What now remains is to connect these Ga−Ga and Ru−Ga bonds to the 14 electron rule for RuGa$_2$.

3. The Band Structure of RuGa$_2$

In an earlier paper, we traced the NCL 14 electron rule to a band gap in the parent structure, RuGa$_2$, at 14 electrons per Ru.[8] We found this gap in both LDA-DFT[16−19] and extended Hückel (eH)[20,21] band structures, in accord with earlier experimental results[11] and better calculations on this structure type.[22−24] These band structures are repeated in Figure 9 where the requisite band gap at 14 electrons per Ru can be clearly seen in both. We now turn to *why* this gap occurs, taking advantage of the simplicity and flexibility of the eH method. The parameters used in these calculations are given in Table 1.

To orient ourselves in this problem, it's convenient to start with the eH density of states (DOS), shown in Figure 10a. The gap at 14 electrons per Ru appears here as a deep hole in the DOS about the E_F. Below this is a dense set of states ranging from about −12 to −17 eV. The high DOS values

(15) Variations of this stacking (different edges over different hexagons) are found in the Si components of the MoSi$_2$ and CrSi$_2$ structures. For a description of this, see ref 4.
(16) Kresse, G.; Hafner, J. *Phys. Rev. B* **1993**, *47*, 55.
(17) Kresse, G.; Hafner, J. *Phys. Rev. B* **1994**, *49*, 14251.
(18) Kresse, G.; Furthmüller, J. *Comput. Mater. Sci.* **1995**, *6*, 15.
(19) Kresse, G.; Furthmüller, J. *Phys. Rev. B* **1996**, *54*, 11169.
(20) Hoffmann, R. *Solids and Surfaces: A Chemist's View of Bonding in Extended Structures;* VCH: New York, 1988.
(21) Landrum, G. A. *YAeHMOP: Yet Another extended Hückel Molecular Orbital Package*, version 2.0b. YAeHMOP is freely available on the WWW at the URL http://sourceforge.net/projects/yaehmop/.
(22) Pécheur, P.; Tobola, J.; Kenzari, H.; Malaman, B.; Welter, R. *J. Alloys Compd.* **2001**, *317−318*, 327−330.
(23) Krajčí, M.; Hafner, J. *J. Phys.: Condens. Matter* **2002**, *14*, 5755−5783.
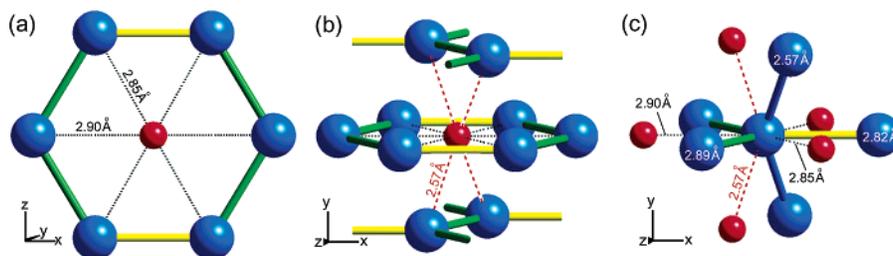(24) Krajčí, M.; Hafner, J. *J. Phys.: Condens. Matter* **2002**, *14*, 7201−7219.

Figure 8. The coordination environments in RuGa$_2$. (a) The Ru–Ga contacts (black dotted lines) within the plane of a Ga honeycomb net. (b) The Ru–Ga contacts (red dotted lines) arising from the stacking of Ga honeycomb nets. (c) The full coordination environment of the Ga atoms. See Figure 4 for the significance of the blue, yellow, and green Ga–Ga bonds.
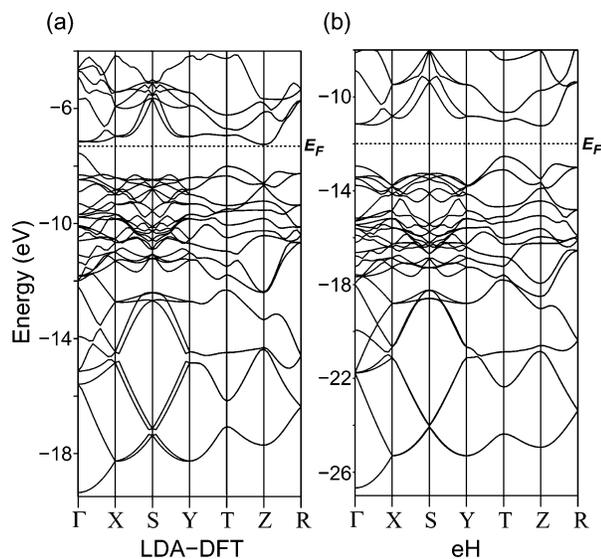

Figure 9. Band structures of the RuGa$_2$ structure type. (a) The band structure calculated for the experimental unit cell, as shown in Figure 2b, with LDA-DFT. (b) The band structure calculated for the idealized structure, as shown in Figure 2c, with the extended Hückel method. The dotted lines give the Fermi energy (E_F) at 14 e$^-$/Ru.

Table 1. Extended Hückel Parameters Used for Transition Metal (T) and Main Group (E) Atom Types

orbital	H_{ii} (eV)	c_1	ζ_1	c_2	ζ_2
T 5s	−10.40		2.08		
T 5p	−6.87		2.04		
T 4d	−14.90	.5340	5.38	.6365	1.80[a]
E 5s	−18.16[b]		2.12		
E 5p	−12.00[c]		1.82		

[a] 2.30 in the standard Ru parameters. [b] −16.16 eV in the standard Sn parameters. [c] −8.32 eV in the standard Sn parameters.

in this region suggest a rather localized set of orbitals, typical of transition metal d bands.[25] This is confirmed with a look at the Ru d portion of the DOS, shown as the shaded region in Figure 10a. The Ru d fills the majority of the curve in the −12 to −17 eV region and dominates the DOS near the E_F. The remainder of the DOS in this curve comes almost entirely from the Ga s and p, suggesting Ru–Ga bonding in this region. This is what is observed in the Ru–Ga crystal orbital overlap population (COOP), shown in Figure 10b. It can also be seen in the Ru–Ga COOP that the gap about the E_F separates Ru–Ga bonding and Ru–Ga antibonding states. Below the Ru d states, there is a tail in the DOS,
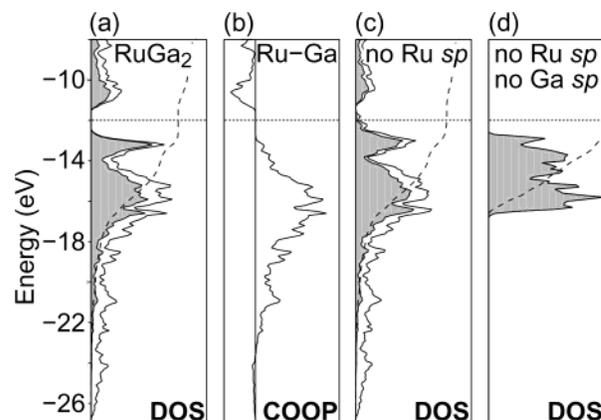

Figure 10. Numerical experiments with the eH electronic structure of RuGa$_2$. (a) eH DOS for the RuGa$_2$ structure. (b) The Ru–Ga COOP for RuGa$_2$. (c) eH DOS for RuGa$_2$ excluding the Ru s and p orbitals. (d) eH DOS for the Ru substructure of RuGa$_2$, excluding both the Ru and Ga sp orbitals. In all DOS curves, the shaded region gives the Ru d projected DOS, with the dashed curves showing the integration of this region. The dotted horizontal lines indicate the eH E_F of RuGa$_2$ for calibration of the energy scale.

running from about −17 to −26 eV. This derives from the Ga s and p. A look at the Ru–Ga COOP reveals that these states are largely Ru–Ga nonbonding (the small negative COOP values near the bottom in this range are the result of counterintuitive orbital mixing[26]).

Let's trim down our eH calculations by taking out orbitals that are unnecessary for the presence of the gap. To do this, we monitor how the eH DOS changes as atomic orbitals are deleted. Our starting point, the total DOS for the full calculation, was shown in Figure 10a. In Figure 10c, we remove the Ru sp levels. The resulting DOS shows some minor changes; for instance, the band gap about E_F has closed slightly from the bottom of the gap to become a deep pseudogap. Overall, however, the correspondence between the calculations with and without the Ru sp is strong. The E_F still lies in a deep hole, implying that the special stability of the 14 electron count remains. For now, we will then leave the Ru sp levels out of our analysis.

In Figure 10d, we remove not only the Ru sp orbitals but also all of the Ga orbitals. We are left with just the Ru d, which occur as a block spread out from about −13 eV to −17 eV. The RuGa$_2$ E_F (dotted line) lies just above this block. This set corresponds to the set of Ru d-rich states in the range of −12 to −17 eV mentioned earlier for the full

(25) Pettifor, D. *Bonding and Structure in Molecules and Solids*; Oxford University Press: Oxford, 1995.

(26) Ammeter, J. H.; Bürgi, H.-B.; Thibeault, J. C.; Hoffmann, R. *J. Am. Chem. Soc.* **1978**, *100*, 3686–3692.
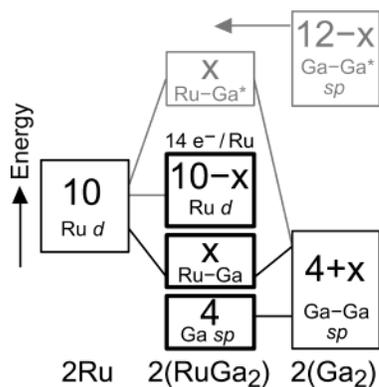
Figure 11. A scheme setting up the problem of the 14 electron rule in $RuGa_2$. For each $RuGa_2$ primitive unit cell, 10 Ru d orbitals interact with $4 + x$ orbitals on the Ga atoms. x is the number of Ga orbitals which form strong interactions with the Ru and, in principle, could depend on the k-point examined. These x interacting Ga levels create bonding and antibonding interactions with x Ru d levels. This leads to 4 Ga, x Ru−Ga, and $10 - x$ Ru levels being filled for 14 occupied orbitals (black, bold boxes), and x unfilled Ru−Ga antibonding orbitals (gray box).

Figure 12. Sampling k-space. (a) The DOS of $RuGa_2$ averaged from a mesh of k-points extending over whole first Brillouin zone. (b) The DOS of $RuGa_2$ averaged from a mesh of k-points lying in the plane shared by the high-symmetry k-points Γ, X, Y, and XY.

calculation (Figure 10a). In $RuGa_2$, this Ru d block is filled, and this is a part of the rationale of the 14 electron count.

4. A Schematic Interaction Diagram

The results of the last section can be summarized with the schematic interaction diagram in Figure 11. We consider two formula units of $RuGa_2$, the contents of the primitive unit cell. The two Ru atoms per unit cell bring 10 d orbitals, while the $2(Ga_2)$ portion brings 16 Ga sp orbitals. Strong interactions occur within the $2(Ga_2)$ portion, as indicated by the multiple Ga−Ga contacts noted in the structure. From this, we anticipate much dispersion in the Ga levels. In the scheme here we simplify this situation by grouping the Ga levels as follows: low-lying Ga−Ga bonding levels (black box), and high-lying Ga−Ga antibonding levels (gray box). There are $4 + x$ low-lying Ga levels, 4 being the minimum number of Ga levels needed to make the 14 occupied orbitals per unit cell.

Here's what happens when we turn on Ru−Ga bonding, which we have seen is important. Of the $4 + x$ low-lying Ga levels, x get involved in Ru−Ga interactions. These combine with the 10 Ru d orbitals to create a 10 below x splitting: x Ru−Ga bonding plus $10 - x$ Ru nonbonding orbitals below a high-lying set of x Ru−Ga antibonding orbitals. The antibonding signature of the last set is found in the Ru−Ga COOP (Figure 10b) above the E_F; the Ru−Ga antibonding levels are unoccupied. Altogether, we are left then with 14 occupied levels per $2(RuGa_2)$: 10 Ru d (and Ru−Ga bonding) plus 4 Ga−Ga bonding, Ru−Ga nonbonding levels. From this, we recover the 14 electrons per Ru atom.

5. Toward the 14 Electron Rule: Limiting k-Points

From the interaction diagram of Figure 11, it is evident that the gap at 14 electrons per Ru rests on the existence of four Ga−Ga bonding/Ru−Ga nonbonding levels per unit cell. How do these arise from the structure of $RuGa_2$? Let's look at the problem k-point by k-point, hoping to find a simple argument that holds across the Brillouin zone.
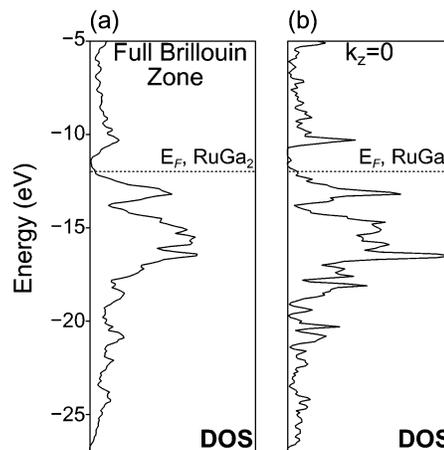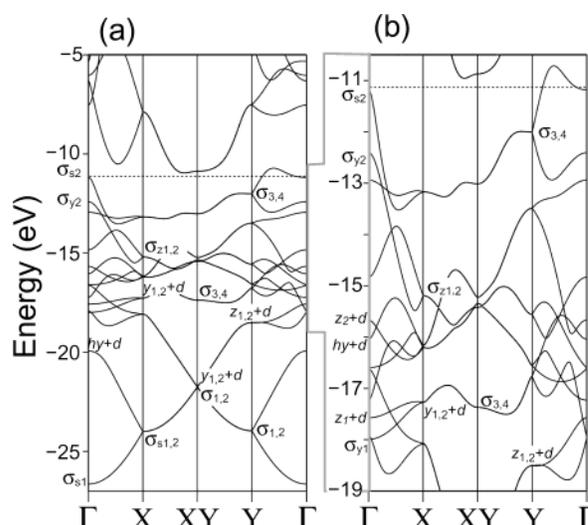

Figure 13. Band structure of the $RuGa_2$ primitive cell between the high-symmetry k-points Γ, X, XY, and Y. For the Ru atoms, only d orbitals are included, following the results shown in Figure 10. (a) All of the occupied bands. (b) A close-up of the Ru d region. See Figures 15, 16, 19, and 20 for descriptions of the band labels.

Which k-points are important? We begin by comparing the DOS of the first Brillouin zone (FBZ) with the DOS of the $(k_x,k_y,0)$ plane (Figure 12). Clearly the latter models the FBZ well. In Figure 13, we show the band structure in this plane. We then focus further on the high symmetry points in this plane: Γ for $\mathbf{k} = (0,0,0)$, X for $\mathbf{k} = (0.5,0,0)$, Y for $\mathbf{k} = (0,0.5,0)$, and XY for $\mathbf{k} = (0.5,0.5,0)$, using the reciprocal lattice for the primitive unit cell of $RuGa_2$ described earlier. At these k-points, the crystal orbitals are real and easy to draw out.

The pivotal four Ga−Ga bonding, Ru−Ga nonbonding levels arise from the Ga portion of the structure, so that's where we begin our analysis at each k-point. First we must identify the $4 + x$ low-lying set (outlined in black on the right side of Figure 11). We do this through the band structure (Figure 14) of the Ga sublattice, assigning the Ga levels below the $RuGa_2$ E_F as belonging to the $4 + x$ set. As can be seen by counting the number of bands below the E_F, x is not a constant. It varies from k-point to k-point, varying
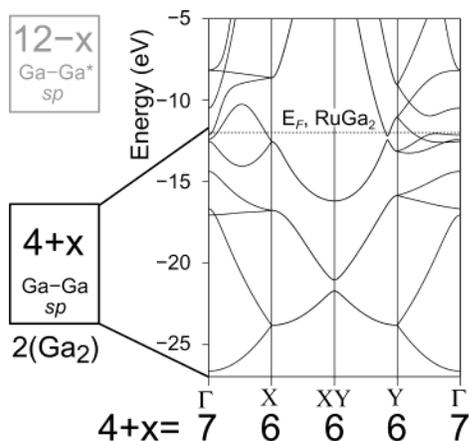
Figure 14. Bands for just the Ga part of the RuGa$_2$ structure, in the plane of the high-symmetry k-points, with reference to the electron counting scheme shown in Figure 11.

from seven low-lying levels at Γ to six at X, XY, and Y (three doubly degenerate bands). To see the distinction between the Ru−Ga nonbonding and the Ru−Ga bonding orbitals, let's now draw out these $4 + x$ Ga orbitals. We will do this at Γ and X, the results being similar at Y and XY, respectively.

6. 14 Electrons per Ru at Γ

As we noted above in Figure 14, the isolated Ga sublattice has seven low-lying crystal orbitals at Γ. Somehow four of them fail to interact effectively with the Ru d levels; we want to understand this in orbital detail. For orientation, we start with a view of the RuGa$_2$ structure (left side of Figure 15a): blue bars indicate the 2.57 Å Ga−Ga contacts, and black dotted lines the 2.82 and 2.89 Å ones. Then, in Figure 15b−e, we overlay the four Ru−Ga nonbonding Ga orbitals onto this framework, assigning labels for the orbitals, which we will refer to when we return to the RuGa$_2$ band structure. Focusing on lobes connected by blue bars, we see why these orbitals are low-lying: all are Ga−Ga bonding along the shortest Ga−Ga contacts. This arises primarily from Ga s−Ga s interactions in $\sigma_{s1,s2}$ and through Ga p−Ga p interactions (involving mainly the Ga p$_y$) in $\sigma_{y1,y2}$. There are four of these shortest Ga−Ga contacts per unit cell, creating the Ga chains we described above. The four levels shown in Figure 15 provide the Ga−Ga σ bonding set for these contacts at Γ.

But why are these levels Ru−Ga nonbonding? To answer this, we focus on the Ga hexagon on the right side of Figure 15a and the Ru atom in its center. On the right side panels of Figure 15b−e, we draw the Ga lobes in the hexagon, abstracted from the full Ga set at left. Let's see how these lobes overlap with the d orbitals of the central Ru atom. The lowest energy Ga orbital, σ_{s1}, has no nodes passing through the Ga hexagon. It would overlap well with a Ru s, but not a d orbital. The next lowest level, σ_{y1}, has one node in the plane of the Ga hexagon; this level has zero overlap with all of the Ru d orbitals. The remaining orbitals, σ_{y2} and σ_{s2}, have no counterpart in the Ru s, p, or d orbitals. All of these orbitals are Ru−Ga nonbonding due to their phasing.

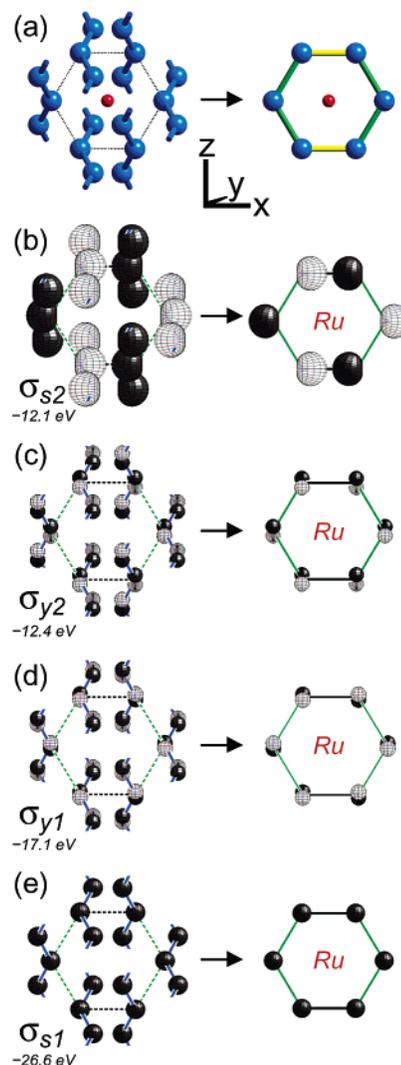Not so for the remaining low-lying Ga levels at Γ. We show these orbitals in Figure 16, in the fashion of Figure

Figure 15. The four Ga−Ga bonding, Ru−Ga nonbonding orbitals at Γ (See Figure 11). Note that these four orbitals are phased in such a way that they do not interact well with the d orbitals of the Ru. (a) A view of the RuGa$_2$ structure for orientation, showing the Ga chains formed from the shortest Ga−Ga contacts in the structure (left) and one hexagon of the honeycomb nets formed from the contacts between chains (right). In the next panels, the orbitals are overlaid on these frames. (b) The orbital we label σ_{s2}, formed from Ga s orbitals bonding along the Ga−Ga contacts along the chain. (c) The σ_{y2} orbital, formed from Ga p$_y$ bonding along the chain. (d) The σ_{y1} orbital. (e) The σ_{s1} orbital. These orbitals are identified in the band structure of Figure 13.

15. Like the previous set of Ga orbitals, these exhibit Ga−Ga bonding, this time along the green contacts, at 2.89 Å. This bonding occurs between Ga p$_z$ orbitals in Figure 16a and Figure 16b, and through hybrids of Ga s and Ga p$_x$ in Figure 16c. But now the overlap with Ru d orbitals is obviously good: for both z$_1$ and z$_2$ orbitals (Figure 16a,b) there is strong overlap with a Ru d$_{xz}$ orbital, with one lobe of the d$_{xz}$ orbital pointing into one of the 2.89 Å Ga−Ga contacts. The result is three-center Ga−Ga−Ru bonding overlap. In the *hy* combination (Figure 16c), the dominant interaction occurs through a σ overlap between the Ga hybrid orbital and a Ru d orbital combining Ru d$_{z^2}$ and d$_{x^2-y^2}$ character.

In the band structure of RuGa$_2$ in Figure 13, we locate the descendants of these Ga orbitals with the labels given to
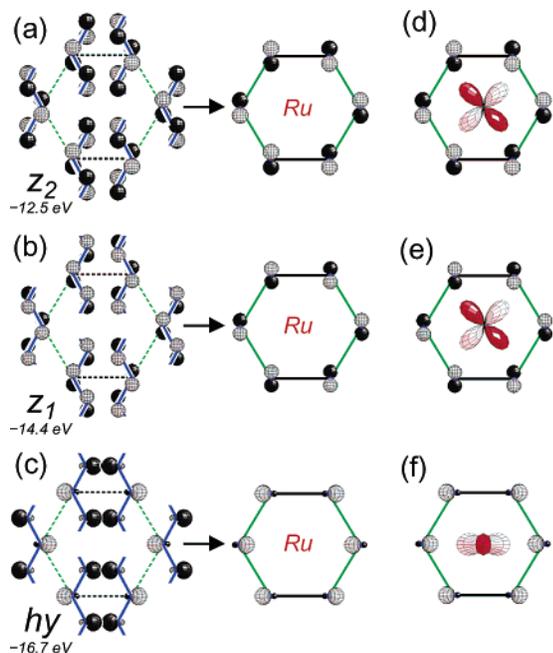
Figure 16. The *x* Ga orbitals ($x = 3$ at Γ) which form Ru−Ga bonds at Γ (see Figure 11). (a) The z_2 orbital, formed from Ga p_z orbitals bonding along the Ga−Ga contacts shown in green. (b) The p_z orbital, formed from Ga p_z bonding along the Ga−Ga contacts. (c) The *hy* orbital, formed from hybrid lobes of Ga s and Ga p_x bonding along the contacts shown in green. These orbitals are identified in the band structure of Figure 13. (d, e, f) The Ru d−Ga overlap for the Ga orbitals of respectively a, b, and c.

the orbitals in Figures 15 and 16. The σ_{s1}, σ_{s2}, σ_{y1}, and σ_{y2} labels indicate the nonbonding Ga levels at Γ, while the *hy* + d, z_1 + d, and z_2 + d labels mark Ru−Ga bonding orbitals. There is significant overlap in energy between the nonbonding Ga levels, Ru−Ga bonding levels, and Ru nonbonding levels. For this reason, it is very difficult to discern these levels in average properties calculations, i.e., COOP or projected DOS analyses, involving the full Brillouin zone.

In summary, here is how the rule of 14 electrons per Ru atom arises at Γ. The Ga−Ga bonding levels (reasonably localized in the chains with the shortest Ga−Ga distances) interact poorly with the Ru d orbitals. As there are four of these contacts per unit cell, four Ga−Ga bonding levels remain at relatively low energy. All of the other low-lying Ga levels interact with the Ru, so a gap occurs after filling the four Ga−Ga levels and the ten Ru d levels (including Ru−Ga bonding, and Ru nonbonding), at 14 electrons per Ru atom.

In terms of classical valence structures at Γ, each atom in the Ga chain forms two two-electron single bonds. Since this uses two electrons, the Ga can be formally written as Ga^+. This classical valence structure is depicted in Figure 17a.

In Figure 18, we anticipate how this scheme will change as we move away from Γ. At X and XY, some of the 2.57 Å Ga−Ga bonding orbitals produce high-energy Ru−Ga antibonding orbitals. In the next section we see that, at X and XY, this is counterbalanced by the appearance of a different set of Ga−Ga bonding, Ru−Ga nonbonding orbitals.

7. 14 Electrons per Ru at X, Y, and XY

At X, the origin of the 14 electron count has both similarities to and differences from that at Γ. There are six low-lying
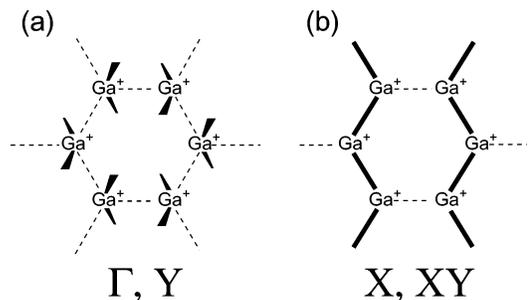

Figure 17. Classical valence structures for Ga^+ in $RuGa_2$. At all four special *k*-points, Ga−Ga bonding occurs along Ga chains. (a) At Γ and Y, the chain bonding occurs along the 2.57 Å contacts. (b) At X and XY, the chain bonding occurs along the 2.89 Å contacts.
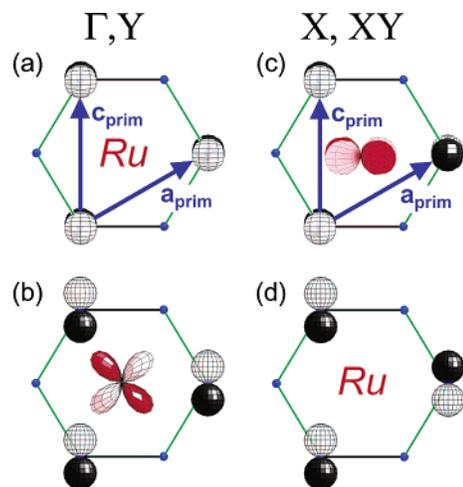

Figure 18. Translational symmetry of the Ga p_y and p_z orbitals, and the Ru−Ga bonding responsible for the shift in Ga−Ga bonding from the 2.57 Å contacts at Γ and Y, to the 2.89 Å contacts at X and XY. At Γ and Y, the orbitals are symmetric with respect to translations along $\mathbf{a}_{prim}$ and $\mathbf{c}_{prim}$. This the makes the (a) Ga p_y and (b) Ga p_z of respectively the wrong and right phasing for overlap with Ru d orbitals. At X and XY, the orbitals are now antisymmetric with respect to $\mathbf{a}_{prim}$ translations. (c) The Ga p_y−Ru d overlap is now favorable, while (d) Ga p_z−Ru d overlap is diminished.

Ga orbitals, compared to seven at Γ. But, as at Γ, there are four Ga−Ga bonding/Ru−Ga nonbonding orbitals with the wrong pseudosymmetries for interacting efficiently with Ru d orbitals. These are shown in Figure 19. The σ_{z1} and σ_{z2} (Figure 19a) are well-suited for a Ru p_z orbital, not a d orbital. Likewise, σ_{s1} and σ_{s2} (Figure 19b) would be expected to overlap strongly with a Ru p_x orbital. The two remaining Ga levels are predisposed to Ru−Ga bonding, and are shown in Figure 20. This set is bonding between Ga−Ga nearest neighbors through the Ga p_y orbitals and has a moderate π overlap with a Ru d_{xy} orbital.

The result of this is that the Ga−Ga overlap in the Ru−Ga nonbonding orbitals is no longer between the shortest Ga−Ga contacts. Instead, the p_z orientation directs the Ga−Ga bonding along the longer 2.89 Å contacts, those represented by green bars in Figure 5b, and which form the "Ga helices". The other Ga−Ga bonding/Ru−Ga nonbonding levels (Figure 19b) are also bonding along this contact, through Ga s−Ga s overlap. As in the Ga−Ga bonding at Γ, there are four of these contacts per unit cell, and four bonding levels, one for each 2.89 Å Ga−Ga bond. The Ga−Ga bonding falls along Ga chains, again suggesting Ga^+ (Figure 17b).
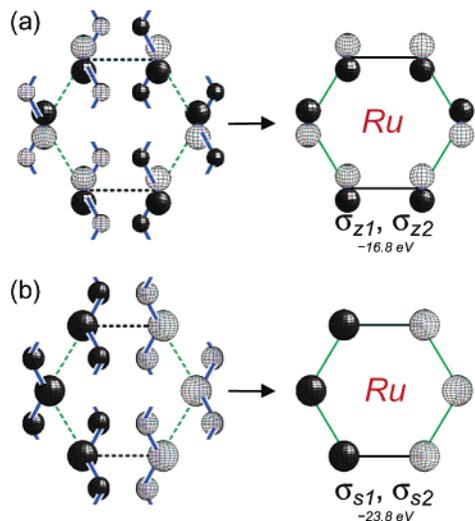
Figure 19. The four Ga−Ga bonding, Ru−Ga nonbonding orbitals at X (See Figure 11). As in the Ru−Ga nonbonding orbitals at Γ, these four orbitals are phased so that they interact poorly with the d orbitals of the Ru. The Ga−Ga bonding here is along the 2.89 Å contacts, not along the shorter 2.57 Å contacts as at Γ. (a) The orbitals labeled σ_{z1} and σ_{z2}, formed from Ga p_z orbitals bonding along the 2.89 Å Ga−Ga contacts (green). (b) The σ_{s1} and σ_{s2} orbitals, formed from Ga s bonding 2.89 Å contacts. These orbitals are identified in the band structure of Figure 13.
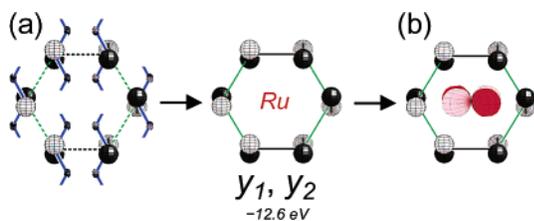

Figure 20. The x Ga orbitals ($x = 2$ at X) which form Ru−Ga bonds at X (see Figure 11). (a) The y_1 and y_2 orbitals, formed from Ga p_y orbitals bonding along the Ga−Ga contacts shown in blue. (b) The Ru d−Ga overlap for this orbital.

In Figure 13, we locate these levels at X in the band diagram of RuGa$_2$, as well as the corresponding levels at Y and XY. At each of these k-points, the 14 electrons per Ru count arises from the filling of four Ga−Ga bonding levels, and 10 Ru d (and Ru−Ga bonding) levels. At Γ and Y, the four Ga−Ga bond levels are due to the four 2.57 Å contacts per unit cell. At X and XY, they come from the four 2.89 Å contacts per cell.

8. Perspectives on the 14 Electron Rule

We found that the 14 electron count in RuGa$_2$ stems from 5 + 2 sets of orbitals per formula unit: five Ru d (and Ru d−Ga bonding) orbitals, plus two Ga orbitals noninteracting with the Ru d. When we looked at different k-points, it became clear that the nature of these Ga orbitals shifts between k-points. For those k-points where translations along $\mathbf{a}_{prim}$ are symmetric (i.e., Γ and Y), the Ga levels consist of bonds along the first nearest-neighbor Ga−Ga contacts. For those k-points where such translations are antisymmetric (i.e., X and XY), the Ga levels consist of bonds along the third nearest-neighbor Ga−Ga contacts. The essential feature for the 14 electron count is that while the type of Ga−Ga bond varies from k-point to k-point, the number of filled Ga−Ga bonding but Ru−Ga nonbonding orbitals remains unchanged.

We may compare the 14 electron rule in RuGa$_2$ with the more familiar 18 electron rule for organometallic transition metal complexes. In Figure 21a we illustrate schematically the origin of the 18 electron rule for a hypothetical transition metal complex TL$_n$, where T is a transition metal and L$_n$ is a complement of n ligands with m donor orbitals ($m \geq n$). The T atom brings nine orbitals: five d, three p, and one s. As we turn on T−L interactions, the m L orbitals combine with m of the nine T orbitals (the assumption is $m \leq 9$). This creates m T−L bonding levels, $9 - m$ T nonbonding orbitals, and m T−L antibonding orbitals. Assuming that all the bonding and nonbonding levels are occupied, there are a total of nine filled levels: m T−L bonding plus 9 - m T nonbonding.[27]

A similar scheme arises for the Ru−Ga bonding in RuGa$_2$, as is shown in Figure 21b, this time for one formula unit of RuGa$_2$. The Ru atom brings five d orbitals to the bonding. The Ga$_2$ portion brings m levels that interact with these Ru d orbitals, and two levels that are primarily limited to Ga−Ga bonding. The persistence of these two levels throughout the whole Brillouin zone (even though, as we saw, they may be involved in different Ga−Ga bonds) gives rise to a band gap at 14 electrons per Ru.

The orbital situation of filled ligand orbitals without transition metal character is well-known in other branches of inorganic chemistry, most notably in organometallic chemistry. In organometallic chemistry, this situation leads to apparent violations of the 18 electron rule. Examples include the formally 20 electron W(PhCCPh)$_3$CO[28−30] and the formally 24 electron Zr(BH$_4$)$_4$.[31] For these compounds (Figure 21c), 18 electrons reside in m T−L bonding and $9 - m$ T nonbonding levels as in normal 18 electron complexes. But most importantly, there is also a group of y orbitals on the ligands which do not overlap (by symmetry) with the metal orbitals. They remain nonbonding and accommodate the remaining electrons. The extra y ligand orbitals in these "18 electron rule violators" play the same role as the two nonbonding Ga levels in RuGa$_2$ we examined in detail in this paper. But while in organometallic chemistry such violators are rare, we see in the Nowotny chimney ladder phases that such behavior is the norm. These results suggest that deviations from the 18 electron rule become more prevalent as main group−main group interactions become more complex. This is the case for transition metal−main group extended solids where the main group atom is the majority component.

9. Conclusions

In this paper, we have continued our study of the 14 electron rule in the Nowotny chimney ladder phases (NCLs), focusing on *why* there is a band gap at 14 electrons per Ru

(27) Albright, T. A.; Burdett, J. K.; Whangbo, M.-H. *Orbital Interactions in Chemistry*; J. Wiley: New York, 1985.
(28) Tate, D. P.; Augl, J. M.; Ritchey, W. M.; Ross, B. L.; Grasselli, J. G. *J. Am. Chem. Soc.* **1964**, *86*, 3261−3265.
(29) King, R. B. *Inorg. Chem.* **1968**, *7*, 1044−1046.
(30) Laine, R. M.; Moriarty, R. E.; Bau, R. *J. Am. Chem. Soc.* **1972**, *94*, 1402−1403.
(31) Hitchcock, A. P.; Hao, N.; Werstiuk, N. H.; McGlinchey, M. J.; Ziegler, T. *Inorg. Chem.* **1982**, *21*, 793−798.
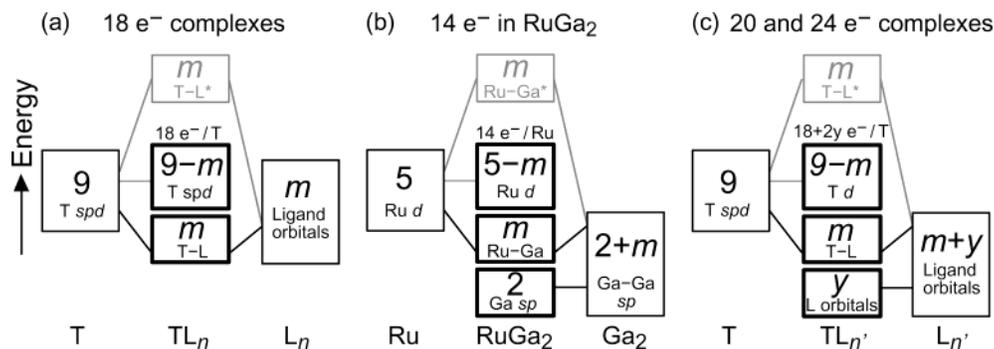
Figure 21. A comparison of the 18 electron rule of transition metal complexes with the 14 electron rule for $RuGa_2$. (a) A schematic interaction diagram for a hypothetical 18 electron complex TL_n, (b) for $RuGa_2$, and (c) for a hypothetical complex $TL_{n'}$ exceeding 18 electrons. The two Ru–Ga nonbonding Ga levels of $RuGa_2$ are analogous to the y T–L nonbonding L orbitals of the $TL_{n'}$ complex.

atom in the parent structure, $RuGa_2$. We found that 10 of the 14 electrons fill the Ru d block, while the remaining 4 occupy Ga orbitals. Fourteen electrons per Ru atom then corresponds to the electron configuration $Ru^{2-}(Ga^+)_2$. The $(Ga^{2+})_2$ component of the structure contains a k-point-dependent balance between bonding along two different sets of Ga chains.

We find that a more general counting scheme is needed to reconcile the 14 and 18 electron rules. In 18 electron compounds, we typically focus on the metal (and metal–ligand bonding) orbitals alone. The remaining ligand orbitals are registered only peripherally, in the ligand Lewis structures. On moving from transition metal complexes to extended solids, we must widen our vision to include these nonbonding orbitals. Only then can we understand the resulting magic electron counts.

One might object, "Why should we worry about arcane electron counting rules of organometallic chemistry in intermetallic extended compounds?" Well, it is all one chemistry, and it is salutary (and satisfying) to look for connections. Which are there.

How does this electron counting scheme for $RuGa_2$ apply to the other NCL phases? As we showed in the first paper of this series,[8] $RuGa_2$ can be used to construct all the other NCLs. In this *Aufbau*, the $RuGa_2$ structure is cut into 2-dimensional slabs. These slabs are then rotated relative to each other by 90° and then fused back together. At the slab interfaces, steric factors force main group atom vacancies. This breaks the Ga–Ga chains—the chains creating the Ga–Ga bonding/Ru–Ga nonbonding orbitals key to our counting scheme (Figure 11). But where Ga–Ga bonds are broken by vacancies, Ga lone pairs appear, and the total number of Ru d–Ga nonbonding Ga orbitals is conserved. Through this mechanism, the stability of the 14 electron count remains. The details of this will be described in a future publication.

As we look beyond the NCL phases themselves, to intermetallic species involving both transition metal and main group atoms, it is clear that high site pseudosymmetry plays an important role. Not only are the transition metal atoms of $RuGa_2$ in a D_2 environment, but hexagons of main group atoms can be perceived around them. With such hexagons of atoms it is possible to prepare fragment orbitals which will interact with a transition metal orbital of s, p, or even f symmetry. And it is of interest to see if such "wrong symmetry" main group orbitals prove a key point in other transition metal main group extended solids.